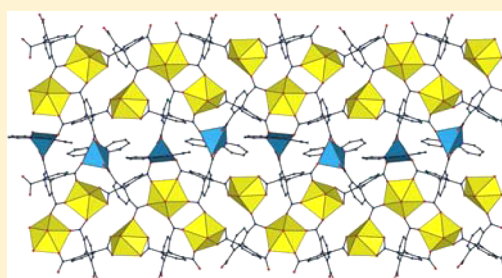


Uranyl Ion Complexes with 1,1'-Biphenyl-2,2',6,6'-tetracarboxylic Acid: Structural and Spectroscopic Studies of One- to Three-Dimensional Assemblies

Pierre Thuéry^{*,†} and Jack Harrowfield^{*,‡}[†]CEA, IRAMIS, CNRS UMR 3685 NIMBE, LCMCE, Bât. 125, 91191 Gif-sur-Yvette, France[‡]ISIS, Université de Strasbourg, 8 allée Gaspard Monge, 67083 Strasbourg, France

S Supporting Information

ABSTRACT: 1,1'-Biphenyl-2,2',6,6'-tetracarboxylic acid (H_4L) was reacted with uranyl nitrate, either alone or in the presence of additional metal cations (Ni^{2+} , Cu^{2+} , Dy^{3+}) under (solvo)-hydrothermal conditions, giving six complexes which were characterized by their crystal structure and, in all but one case, their emission spectrum in the solid state. $[Ni(bipy)_3][UO_2(H_2L)(H_2O)_2](NO_3)_2 \cdot 3H_2O$ (**1**) crystallizes as a one-dimensional (1D), ribbon-like coordination polymer, while the homometallic complex $[(UO_2)_2(L)(H_2O)_3] \cdot H_2O \cdot CH_3CN$ (**2**) and the heterometallic complexes $[UO_2Cu(L)(H_2O)_2] \cdot H_2O$ (**3**), $[UO_2Cu(L)(H_2O)] \cdot H_2O$ (**4**), and $[(UO_2)_5Cu_4(HL)_6(bipy)_4] \cdot 2H_2O$ (**5**) display two-dimensional (2D) arrangements. Lastly, the uranyl–lanthanide heterometallic complex $[(UO_2)_8Dy(HL)_6(H_2O)_8](I) \cdot 8H_2O$ (**6**) crystallizes as a three-dimensional (3D) framework. Although these assemblies adopt different topologies, the $\{4^2.6\}$ linear motif found in **1** is discernible in the structures of **2**, **5**, and **6**, in which the higher dimensionality arises from further bridging of these subunits by uranyl (**2**), copper (**5**), or both uranyl and dysprosium (**6**) cations. The tetracarboxylic/ate ligands have their two aromatic rings nearly perpendicular to one another. No two of them adopt the same coordination mode in this series (except in the similar complexes **3** and **4**), but chelation involving one carboxylate group from each ring is nearly ubiquitous, and the ensuing position of the cation favors the formation of planar architectures. The emission spectra of complexes **2**–**5** measured in the solid state show the usual uranyl vibronic fine structure, although with significant differences in the emission intensity, while complete quenching of the luminescence is observed in **1**.



■ INTRODUCTION

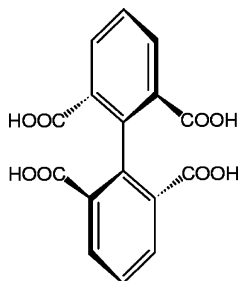
Uranyl–organic coordination polymers or frameworks involving carboxylate ligands have been shown to display a great variety of architectures, in spite of the geometric limitations inherent to the linear uranyl cation, and their photophysical properties elicited particular interest.¹ Although their synthesis has made frequent use of benzene polycarboxylates,² syntheses based on the biphenyl platform have been much less investigated, the main reason probably being that few such ligands are commercially available. The simplest symmetrically disubstituted species, 1,1'-biphenyl-4,4'-dicarboxylic acid, has been shown to give a two-dimensional (2D) assembly analogous to that obtained with 1,4-benzenedicarboxylic acid,^{2g} a different 2D assembly comprising additional hydroxide ligands, and even a three-dimensional (3D) framework.³ Another 3D architecture was obtained with 1,1'-biphenyl-2,2'-dinitro-4,4'-dicarboxylic acid,⁴ while with 1,1'-biphenyl-3,3',4,4'-tetracarboxylic acid, two carboxylic acid groups are uncoordinated, and the coordination polymer formed is one-dimensional (1D).⁵ A few examples have been reported also with polycarboxylates based on bipyridyl⁵ or terphenyl⁶ platforms. Biphenyl-based ligands are of particular interest because of the tilting of the two aromatic rings with respect to

one another, thus providing an alternative to the inherent planarity of the benzene-based ligands. This could be expected to significantly modify their uranyl ion coordination chemistry since the building of nonplanar uranyl–organic assemblies largely relies on the ability of the ligand to provide the required connectivity out of the uranyl equatorial plane, and the carboxylate unit is, of course, particularly versatile in regard to its coordination mode (unidentate, bidentate, bridging bidentate, syn- and anti-lone pair binding). With this in view, we turned to 1,1'-biphenyl-2,2',6,6'-tetracarboxylic acid (H_4L , Scheme 1), in which the two aromatic rings are necessarily nearly orthogonal to one another as a result of steric hindrance between the functional groups.⁷ This molecule has been used as a building block in combinatorial chemistry,⁸ a hydrogen bonding tecton,^{7b,9} and also a ligand in metal complexes, particularly with alkaline-earth¹⁰ and d- or p-block cations,¹¹ with only one example reported recently with a 4f metal cation, La^{3+} .¹² In the latter case, a 3D framework was obtained, but different arrangements are to be expected for the 5f uranyl cation, due to the peculiar geometrical requirements of this

Received: March 16, 2015

Published: June 23, 2015



Scheme 1. 1,1'-Biphenyl-2,2',6,6'-tetracarboxylic Acid (H_4L)

linear species. In the present work, this ligand was reacted with uranyl ions under hydro- or solvo-hydrothermal conditions (with acetonitrile or *N*-methyl-2-pyrrolidone as organic components), either alone or in the presence of additional reactants (3d-block or 4f metal cations, 2,2'-bipyridine). Such variation of the solvent and the additional species present was intended as a way to generate different complexes with possibly varying dimensionalities, and it permitted indeed the synthesis of six complexes which crystallize as 1D, 2D, or 3D architectures, and which were characterized by determination of their crystal structures and, in all but one case, their emission spectra at ambient temperature.

EXPERIMENTAL SECTION

Synthesis. Uranium is a radioactive and chemically toxic element, and uranium-containing samples must be handled with suitable care and protection.

1,1'-Biphenyl-2,2',6,6'-tetracarboxylic acid (H_4L) was synthesized as previously reported.⁸ $UO_2(NO_3)_2 \cdot 6H_2O$ (depleted uranium, R. P. Normapur, 99%) and $Ni(NO_3)_2 \cdot 6H_2O$ were purchased from Prolabo, $Cu(NO_3)_2 \cdot 2.5H_2O$ and $Dy(NO_3)_3 \cdot xH_2O$ were from Aldrich, and 2,2'-

bipyridine (bipy) was from Fluka. Elemental analyses were performed by MEDAC Ltd. at Chobham, U.K.

$[Ni(bipy)_3][UO_2(H_2L)(H_2O)]_2(NO_3)_2 \cdot 3H_2O$ (**1**). H_4L (17 mg, 0.05 mmol), $UO_2(NO_3)_2 \cdot 6H_2O$ (25 mg, 0.05 mmol), $Ni(NO_3)_2 \cdot 6H_2O$ (15 mg, 0.05 mmol), 2,2'-bipyridine (16 mg, 0.10 mmol), and demineralized water (0.8 mL) were placed in a 10 mL tightly closed glass vessel and heated at 140 °C under autogenous pressure, giving light yellow crystals of complex **1** within 4 days (8 mg, 17% yield). Anal. Calcd for $C_{62}H_{50}N_8NiO_{31}U_2$: C, 38.43; H, 2.60; N, 5.78. Found: C, 37.74; H, 2.38; N, 5.50%.

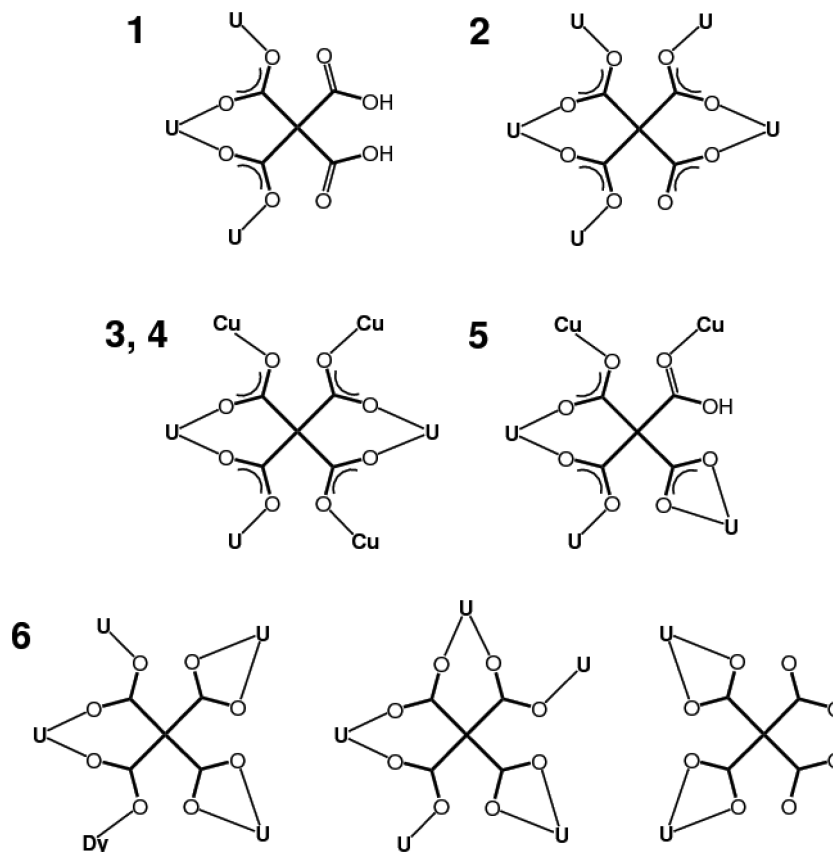
$[UO_2)_2(L)(H_2O)_3] \cdot H_2O \cdot CH_3CN$ (**2**). H_4L (17 mg, 0.05 mmol), $UO_2(NO_3)_2 \cdot 6H_2O$ (50 mg, 0.10 mmol), acetonitrile (0.3 mL), and demineralized water (0.7 mL) were placed in a 10 mL tightly closed glass vessel and heated at 140 °C under autogenous pressure, giving light yellow crystals of complex **2** overnight (18 mg, 37% yield). The acetonitrile molecules are partly lost upon washing with water and drying, and the best match for the analysis corresponds to $\sim 0.5 CH_3CN$. Anal. Calcd for $C_{17}H_{15.5}N_{0.5}O_{16}U_2$: C, 21.29; H, 1.63; N, 0.73. Found: C, 21.15; H, 1.70; N, 0.49%.

$[UO_2Cu(L)(H_2O)_2] \cdot H_2O$ (**3**). H_4L (17 mg, 0.05 mmol), $UO_2(NO_3)_2 \cdot 6H_2O$ (25 mg, 0.05 mmol), $Cu(NO_3)_2 \cdot 2.5H_2O$ (12 mg, 0.05 mmol), acetonitrile (0.3 mL), and demineralized water (0.7 mL) were placed in a 10 mL tightly closed glass vessel and heated at 140 °C under autogenous pressure, giving light yellow-green crystals of complex **3** within 10 days (12 mg, 34% yield). The analysis indicates possible hydration of the sample, in excess of that given by structure determination (see below). Anal. Calcd for $C_{16}H_{12}CuO_{13}U + H_2O$: C, 26.26; H, 1.93. Found: C, 26.27; H, 1.83%.

$[UO_2Cu(L)(H_2O)] \cdot H_2O$ (**4**). H_4L (17 mg, 0.05 mmol), $UO_2(NO_3)_2 \cdot 6H_2O$ (25 mg, 0.05 mmol), $Cu(NO_3)_2 \cdot 2.5H_2O$ (12 mg, 0.05 mmol), *N*-methyl-2-pyrrolidone (NMP, 0.2 mL), and demineralized water (0.6 mL) were placed in a 10 mL tightly closed glass vessel and heated at 140 °C under autogenous pressure, giving light yellow-green crystals of complex **4** within 10 days (24 mg, 69% yield). The analysis indicates retention of a small amount of NMP, in spite of washing with water and drying. Anal. Calcd for $C_{16}H_{10}CuO_{12}U + 0.25NMP$: C, 28.75; H, 1.71; N, 0.49. Found: C, 28.53; H, 1.96; N, 1.13%.

Table 1. Crystal Data and Structure Refinement Details

	1	2	3	4	5	6
chemical formula	$C_{62}H_{50}N_8NiO_{31}U_2$	$C_{18}H_{17}NO_{16}U_2$	$C_{16}H_{12}CuO_{13}U$	$C_{16}H_{10}CuO_{12}U$	$C_{136}H_{78}Cu_4N_8O_{60}U_5$	$C_{96}H_{74}DyIO_{80}U_8$
<i>M</i> (g mol ⁻¹)	1937.87	979.39	713.83	695.81	4228.37	4701.19
cryst syst	monoclinic	triclinic	monoclinic	orthorhombic	monoclinic	monoclinic
space group	$P2_1/n$	$P\bar{1}$	$P2_1/n$	$Pbca$	$P2_1/c$	$C2/c$
<i>a</i> (Å)	10.6421(4)	9.0667(3)	9.3067(9)	16.1517(5)	17.1003(4)	30.5301(7)
<i>b</i> (Å)	25.1317(16)	10.4968(5)	15.5727(15)	15.3424(4)	14.9120(5)	15.9030(7)
<i>c</i> (Å)	25.4129(16)	13.9008(7)	14.1472(12)	16.5323(5)	25.7571(8)	29.9686(10)
α (deg)	90	72.739(2)	90	90	90	90
β (deg)	91.853(4)	73.394(3)	93.923(7)	90	94.538(2)	107.986(2)
γ (deg)	90	67.672(3)	90	90	90	90
<i>V</i> (Å ³)	6793.2(7)	1146.01(9)	2045.6(3)	4096.8(2)	6547.5(3)	13839.3(8)
<i>Z</i>	4	2	4	8	2	4
<i>D</i> _{calcd} (g cm ⁻³)	1.895	2.838	2.318	2.256	2.145	2.256
μ (Mo <i>K</i> α) (mm ⁻¹)	5.127	14.198	9.013	8.994	6.902	10.182
<i>F</i> (000)	3752	888	1332	2584	4012	8580
reflns collcd	188967	67336	67389	141032	216643	245741
indep reflns	12848	6979	3881	3880	12386	13110
obsd reflns [<i>I</i> > 2 σ (<i>I</i>)]	9058	6114	3164	3171	10445	10363
<i>R</i> _{int}	0.101	0.039	0.037	0.021	0.035	0.034
params refined	982	335	280	316	1018	901
<i>R</i> ₁	0.075	0.033	0.087	0.064	0.044	0.049
<i>wR</i> ₂	0.195	0.093	0.270	0.176	0.098	0.147
<i>S</i>	1.178	1.090	1.138	1.084	1.174	1.060
$\Delta\rho_{min}$ (e Å ⁻³)	-1.02	-3.10	-3.05	-2.35	-1.50	-3.93
$\Delta\rho_{max}$ (e Å ⁻³)	1.87	1.72	6.53	1.91	2.54	2.86

Scheme 2. Coordination Modes of the Tetracarboxylic/ate Ligands in Complexes 1–6^a

^aThe ligand is viewed along the central bond. The location of the carboxylic protons in **6** is unknown.

$[(\text{UO}_2)_5\text{Cu}_4(\text{HL})_6(\text{bipy})_4]\cdot 2\text{H}_2\text{O}$ (**5**). H_4L (17 mg, 0.05 mmol), $\text{UO}_2(\text{NO}_3)_2\cdot 6\text{H}_2\text{O}$ (25 mg, 0.05 mmol), $\text{Cu}(\text{NO}_3)_2\cdot 2.5\text{H}_2\text{O}$ (12 mg, 0.05 mmol), 2,2'-bipyridine (16 mg, 0.10 mmol), and demineralized water (0.7 mL) were placed in a 10 mL tightly closed glass vessel and heated at 140 °C under autogenous pressure, giving dark green crystals of complex **5** within 1 week (9 mg, 26% yield). Anal. Calcd for $\text{C}_{136}\text{H}_{78}\text{Cu}_4\text{N}_8\text{O}_{60}\text{U}_5$: C, 38.63; H, 1.86; N, 2.65. Found: C, 38.06; H, 1.91; N, 2.52%.

$[(\text{UO}_2)_8\text{Dy}(\text{HL})_6(\text{H}_2\text{O})_8]\cdot 8\text{H}_2\text{O}$ (**6**). H_4L (17 mg, 0.05 mmol), $\text{UO}_2(\text{NO}_3)_2\cdot 6\text{H}_2\text{O}$ (25 mg, 0.05 mmol), $\text{Dy}(\text{NO}_3)_3\cdot x\text{H}_2\text{O}$ (35 mg, 0.10 mmol on an anhydrous basis), and demineralized water (0.8 mL) were placed in a 10 mL tightly closed glass vessel and heated at 140 °C under autogenous pressure, giving light yellow crystals of complex **6** in very low yield within 1 week. The yield was not improved upon prolonged heating.

Crystallography. The data were collected at 150(2) K on a Nonius Kappa-CCD area detector diffractometer¹³ using graphite-monochromated Mo $K\alpha$ radiation ($\lambda = 0.71073$ Å). The crystals were introduced into glass capillaries with a protective coating of Paratone-N oil (Hampton Research). The unit cell parameters were determined from 10 frames, then refined on all data. The data (combinations of φ - and ω -scans with a minimum redundancy of 4 for 90% of the reflections) were processed with HKL2000.¹⁴ Absorption effects were corrected empirically with the program SCALEPACK.¹⁴ The structures were solved by intrinsic phasing with SHELXT¹⁵ (Patterson map interpretation for complex **2**), expanded by subsequent difference Fourier synthesis and refined by full-matrix least-squares on F^2 with SHELXL-2014.¹⁶ All non-hydrogen atoms were refined with anisotropic displacement parameters. The hydrogen atoms bound to oxygen atoms were found on difference Fourier maps, except in some cases (see Supporting Information), and the carbon-bound hydrogen atoms were introduced at calculated positions. All hydrogen atoms were treated as riding atoms with an isotropic displacement parameter

equal to 1.2 times that of the parent atom (1.5 for CH_3 in **2**, with optimized geometry). Because of low crystal quality and disorder, the refinement of several of the structures, particularly those of **1**, **3**, and **4**, was not very satisfying, and restraints had to be applied on some bond lengths, angles, and displacement parameters, particularly in the disordered or badly resolved parts in all compounds. Special details for each compound are given as Supporting Information. Crystal data and structure refinement parameters are given in Table 1. The molecular plots were drawn with ORTEP-3¹⁷ and the polyhedral representations with VESTA.¹⁸ The topological analyses were done with TOPOS.¹⁹

Luminescence Measurements. Emission spectra were recorded on solid samples using a Horiba-Jobin-Yvon Fluorolog spectrofluorometer. The powdered complex was pressed between two silica plates which were mounted such that the faces were oriented vertically and at 45° to the incident excitation radiation. An excitation wavelength of 420 nm was used in all cases and the emissions monitored between 450 and 650 nm.

Infrared Spectroscopy. IR spectra were recorded on the crystalline samples using a Nicolet 6700 FTIR instrument with a Smart Orbit diamond-anvil attachment.

RESULTS AND DISCUSSION

Synthesis and Characterization. Complexes **1–6** were synthesized under either purely hydrothermal (**1**, **5**, and **6**) or solvo-hydrothermal (**2–4**) conditions at 140 °C (a value in the middle of the range of temperatures commonly employed). All crystals appeared during the heating phase, and their presence in the glass vials was checked visually. In the case of solvo-hydrothermal conditions, the solvent used was either acetonitrile in **2** and **3** or *N*-methyl-2-pyrrolidone (NMP) in **4**, but only in the case of **2** is it present, as a lattice solvent, in the final product. Additional metal cations were introduced in

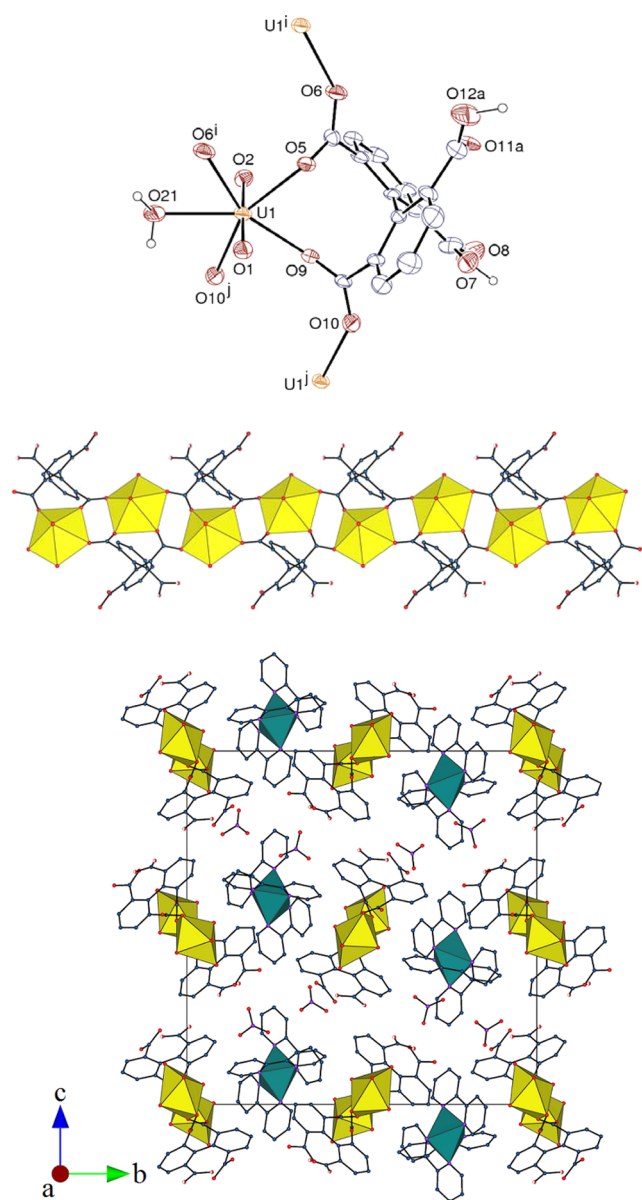


Figure 1. Top: View of complex **1**. Displacement ellipsoids are drawn at the 30% probability level. Only one of the two independent moieties and one position of the disordered parts are represented. Counterions, solvent molecules and carbon-bound hydrogen atoms are omitted. Symmetry codes: $i = 1 - x, 1 - y, 2 - z$; $j = 2 - x, 1 - y, 2 - z$. Middle: View of the 1D assembly. Bottom: View of the packing with chains viewed end-on. The uranium coordination polyhedra are yellow and those of nickel are green. Solvent molecules and hydrogen atoms are omitted in the last two views.

some of the syntheses, Ni^{2+} (**1**), Cu^{2+} (**3–5**), or Dy^{3+} (**6**), and in all cases, they are part of the final species, either as a counterion (**1**) or as a component of a heterometallic complex (**3–6**). 2,2'-Bipyridine (bipy) was added in two of the syntheses (**1** and **5**), and it is bound to the 3d-block metal cation in both cases, but although the stoichiometry of the reactants is the same, a $[\text{Ni}(\text{bipy})_3]^{2+}$ counterion is formed in **1**, while $\text{Cu}(\text{bipy})^{2+}$ is incorporated into the coordination polymer in **5**. The presence of iodide ions in **6** is possibly due to some impurity in the ligand, the synthesis⁸ involving the use of a very large excess of sodium periodate. The violet color of iodine vapor was observed in the reaction vessel during the heating

phase, and the oxidation of iodide, presumably by the nitrate ion also present, may explain the low yield of the crystalline product. An interesting aspect of this family of complexes is related to the deprotonation degree of the tetracarboxylic acid. While polycarboxylates are most often completely deprotonated when reacted with uranyl ions in conditions similar to those used here (with no added base in most cases), three different states are observed in the present series, H_2L^{2-} in **1**, HL^{3-} in **5** and **6**, and L^{4-} in **2–4**. It is notable that complete ionization is achieved only in the cases in which solvo-hydrothermal conditions were used. These differences are presumably the consequences of a complicated interaction of solution ionization and complexation equilibria with solubility equilibria. Elemental analyses were consistent with the compositions deduced from the crystal structures (described below), and the IR spectra (Supporting Information), all rather similar, showed the expected features for the species present, in particular a strong uranyl unit absorption at $930 \pm 5 \text{ cm}^{-1}$.

Crystal Structures. One of the most salient, and unfortunate, characteristics of these complexes is the presence of important disorder phenomena in the solid state (see Supporting Information), with often the added (and possibly related) drawback of poor crystal quality. The disordered parts have been modeled as could best be done, but the large and very anisotropic displacement parameters observed in some parts of the structures show that further, unresolved disorder may be present. It appears that the disorder is most often due to rotation of $\text{COO}(\text{H})$ groups with respect to the aromatic ring, which may involve an uncoordinated group, as in **1**, or be associated with the presence of two close positions or partial occupancy of the bonded metal cation (**4** and **5**). Only in the homometallic complex **2** are these problems altogether absent. Although the overall shape of the ligand is retained within this series of compounds, the dihedral angle between the two aromatic rings displays significant variation within the range $72.1(4)–90.0(3)^\circ$, the smallest values being found in complexes **1** and **2** and the largest in **5** and **6**. The dihedral angles between the $\text{COO}(\text{H})$ groups and the aromatic rings vary much more widely, being in the $3.0(9)–86.5(3)^\circ$ range, thus covering all the possible geometries, from parallel to orthogonal, showing that steric hindrance is not such as to prevent rotational freedom of the functional groups. A search of the Cambridge Structural Database (CSD, version 5.35)²⁰ gives 52 crystal structures containing the H_4L molecule or any of its anions, and the dihedral angles between the aromatic rings are in the $61.8–90^\circ$ range, while those between the carboxylic/ate groups and the aromatic rings span the range from 1.4 to 86.9° , with the relative values in any single molecule following no particular obvious trend (except that, whereas all four angles may assume small values, there is no case of more than one nearly orthogonal COO group). The present values are thus unexceptional, but, together with the large number of coordination sites and various degrees of deprotonation, they justify anticipation of some variability in the coordination modes, as indeed has been found (Scheme 2).

The asymmetric unit in the complex $[\text{Ni}(\text{bipy})_3][\text{UO}_2(\text{H}_2\text{L})(\text{H}_2\text{O})_2(\text{NO}_3)_2 \cdot 3\text{H}_2\text{O}]$ (**1**) contains two uranyl ions in similar environments. Each uranium atom is chelated between two carboxylate groups from the two rings of one ligand, a coordination mode which will be denoted as mode 2, by contrast to chelation by one carboxylate group (mode 1). The five-coordinate equatorial environment is completed by two monodentate carboxylate groups from two other ligands

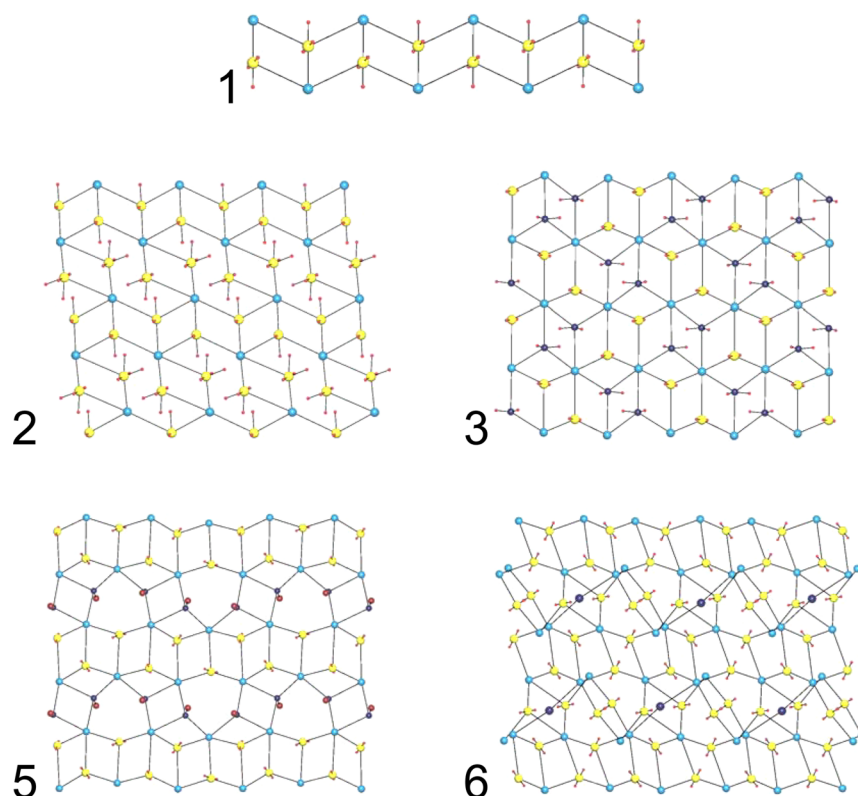


Figure 2. Nodal representations of the 1D assembly in **1**, of the 2D networks in complexes **2** (down the $[1\ 0\ 1]$ axis with the $[0\ 1\ 0]$ horizontal), **3** (down $[1\ 0\ 1]$ with the $[0\ 1\ 0]$ vertical), and **5** (down $[1\ 0\ 0]$ with the $[0\ 1\ 0]$ vertical), and of the 3D framework in **6** (down $[0\ 1\ 0]$ with the $[1\ 0\ 0]$ horizontal). The topology of the network in **4** is similar to that in **3**. Yellow, uranium; dark blue, copper or dysprosium; red, oxygen; light blue, centroid of the L^{4-} ligand; dark red, centroid of the bipy ligand.

and a water molecule to give a pentagonal bipyramidal uranium environment (Figure 1). The U–O(carboxylate) bond lengths are in the range 2.339(8)–2.426(8) Å [average 2.38(3) Å]. The ligand is bonded to the metal ion through one carboxylate group from each aromatic ring only, the coordination mode being bridging bidentate, and it thus connects three cations. 1D ribbon-shaped coordination polymers parallel to $[1\ 0\ 0]$ and containing either U1 or U2 and their symmetry equivalents are formed, which display a central row of doubly bridged cations and the uncoordinated carboxylic acid groups located on either edge. These chains have the total point (Schläfli) symbol $\{4^2.6\}$, and one of them is shown in nodal form in Figure 2. The two carboxylic acid groups (one of them disordered) are involved in hydrogen bonds with either lattice water solvent molecules or nitrate ions $[O\cdots O$ distances and $O-H\cdots O$ angles in the ranges 2.62(2)–3.325(17) Å and 129–157°, respectively]. The coordinated water molecules are hydrogen bonded either to a carboxylic group from the same chain or to lattice solvent water molecules or nitrate ions $[O\cdots O$ distances and $O-H\cdots O$ angles in the ranges 2.84(2)–3.48(4) Å and 133–156°, respectively]. It is notable that these chains are neutral, so that the charge of $[\text{Ni}(\text{bipy})_3]^{2+}$ is balanced by that of the two nitrate anions. The packing displays alternate layers of uranyl-containing chains and nickel-containing cations parallel to $(0\ 1\ 0)$. Although there is no significant parallel π -stacking, $\text{CH}\cdots\pi$ interactions are seemingly present, between either one hydrogen atom of H_2L^{2-} and one aromatic ring of bipy, or between hydrogen atoms of bipy and aromatic rings of bipy or H_2L^{2-} [$\text{H}\cdots\text{centroid}$ 2.83–2.98 Å, $\text{C}-\text{H}\cdots\text{centroid}$ 120–155°].

The asymmetric unit in complex $[(\text{UO}_2)_2(\text{L})(\text{H}_2\text{O})_3]\cdot\text{H}_2\text{O}\cdot\text{CH}_3\text{CN}$ (**2**) contains two uranyl ions in different environments (Figure 3). Both of them are chelated in mode 2 by the same ligand, but U1 is bound to two monodentate carboxylate groups from two other ligands and one water molecule, and U2 to one carboxylate group and two water molecules. The U–O(carboxylate) bond lengths are in the range 2.335(5)–2.407(4) Å [average 2.37(2) Å]. U1 and U2 are thus 3- and 2-fold nodes, respectively, and the L^{4-} ligand is a 5-fold one since one of the oxygen atoms (O8) is uncoordinated. This results in the formation of a 2D assembly parallel to $(1\ 0\ 1)$ with the point symbol $\{4^2.6\}\{4^3.6.8^4.10^2\}\{4\}$ (successive symbols for U1, L^{4-} and U2, respectively), which is represented in nodal form in Figure 2. Two kinds of alternate rows run along the $[0\ 1\ 0]$ axis: one of them, containing U1 and its symmetry equivalents, contains a continuous set of doubly bridged uranyl ions, while the other, corresponding to U2, displays isolated doubly bridged dimers. These rows are connected to one another by L^{4-} ligands arranged in a staggered fashion. It is notable that the main axis of the ligand, bisecting the two aromatic rings, is nearly perpendicular to the sheet plane, so that the tips of the aromatic rings are directed outward on either side, the sheets being tightly packed in bump-to-hollow fashion. The water ligands are involved in hydrogen bonds with a variety of acceptors, an uranyl oxo group, carboxylate groups, and other water ligands, all in the same sheet, as well as lattice water and acetonitrile molecules $[O\cdots O/N$ distances and $O-H\cdots O/N$ angles in the ranges 2.716(8)–3.125(7) Å and 124–164°, respectively].

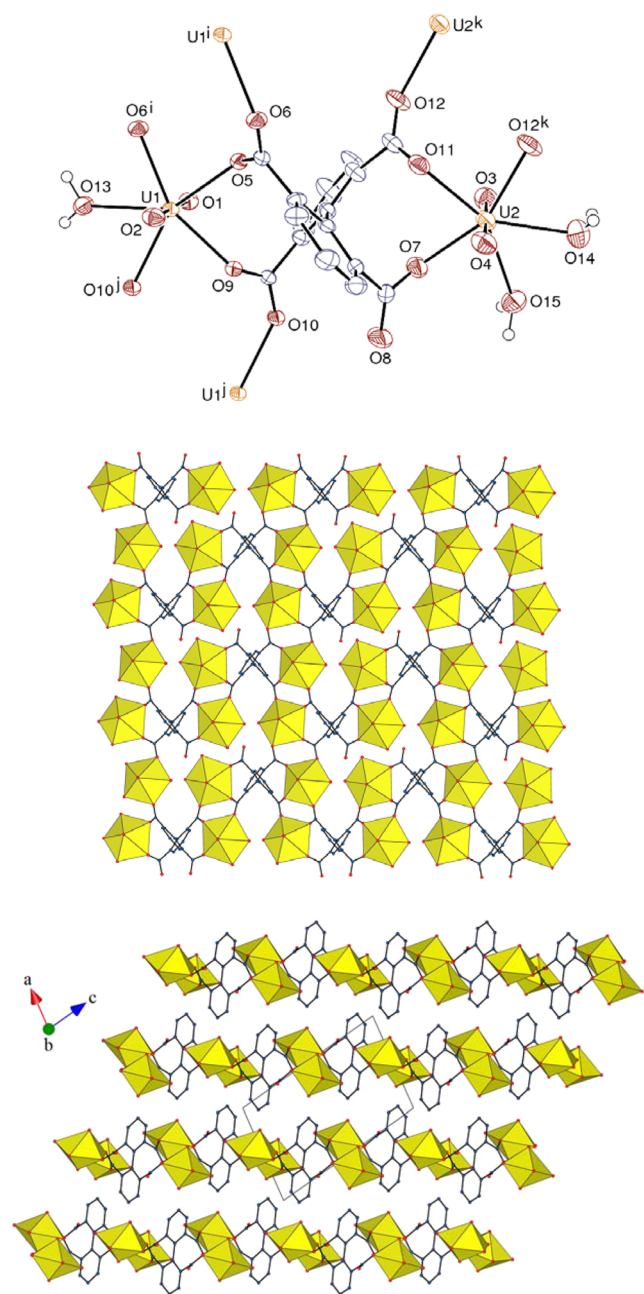


Figure 3. Top: View of complex **2**. Displacement ellipsoids are drawn at the 50% probability level. Solvent molecules and carbon-bound hydrogen atoms are omitted. Symmetry codes: $i = 1 - x, 1 - y, 2 - z$; $j = 1 - x, -y, 2 - z$; $k = 2 - x, 1 - y, 1 - z$. Middle: View of the 2D assembly. Bottom: View of the packing with layers viewed edge-on. Solvent molecules and hydrogen atoms are omitted in the last two views.

Reaction of a mixture of uranyl and copper(II) nitrates in water/acetonitrile gives the complex $[\text{UO}_2\text{Cu}(\text{L})(\text{H}_2\text{O})_2] \cdot \text{H}_2\text{O}$ (**3**). The uranyl ion is chelated in mode 2 by two L^{4-} ligands and is bound to a monodentate carboxylate from a third ligand (Figure 4). The $\text{U}-\text{O}(\text{carboxylate})$ bond lengths are as usual $[2.355(13)–2.413(13) \text{ \AA}]$, average $2.38(2) \text{ \AA}$. Among the four carboxylate oxygen atoms which are not involved in chelation, only one is bound to uranium, the other three being coordinated to copper atoms. The Cu^{2+} cation is in an axially elongated square pyramidal environment, with the carboxylate donors $\text{O}4^k$ and $\text{O}5$ and two water molecules defining the basal

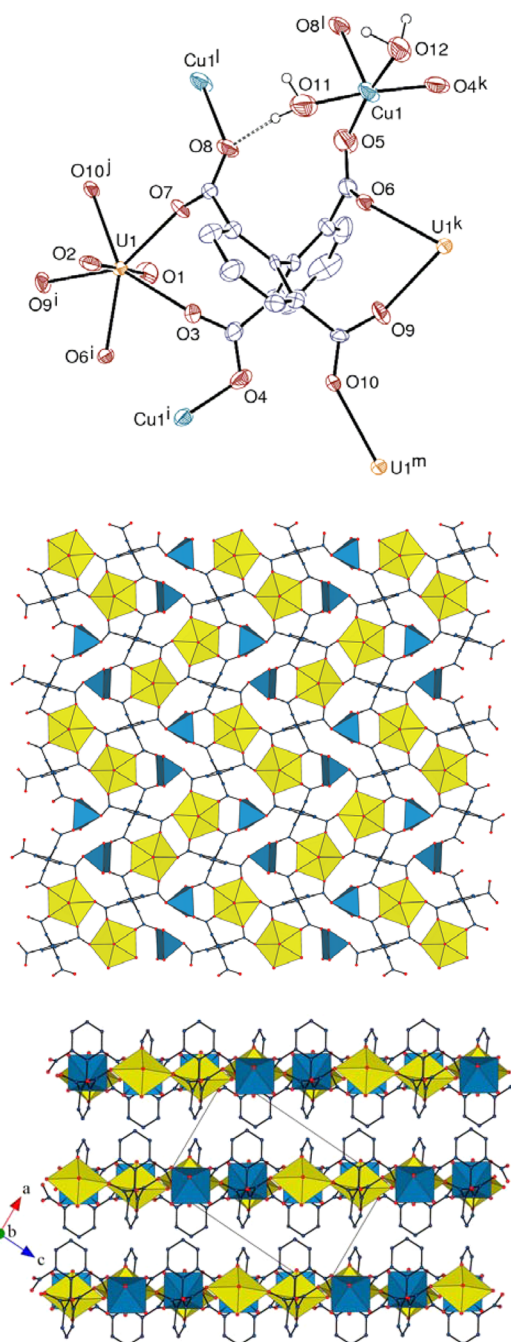


Figure 4. Top: View of complex **3**. Displacement ellipsoids are drawn at the 30% probability level. The solvent molecule and carbon-bound hydrogen atoms are omitted. The hydrogen bond is shown as a dashed line. Symmetry codes: $i = x + 1/2, 1/2 - y, z + 1/2$; $j = 3/2 - x, y + 1/2, 3/2 - z$; $k = x - 1/2, 1/2 - y, z - 1/2$; $l = 1 - x, 1 - y, 1 - z$; $m = 3/2 - x, y - 1/2, 3/2 - z$. Middle: View of the 2D assembly. Bottom: View of the packing with layers viewed edge-on. The uranium coordination polyhedra are yellow and those of copper are blue. Solvent molecules and hydrogen atoms are omitted in the last two views.

plane $[\text{Cu}1-\text{O} \text{ bond lengths in the range } 1.94(3)–1.99(2) \text{ \AA}]$, and the carboxylate atom $\text{O}8^l$ in the axial position $[\text{Cu}1-\text{O}8^l 2.195(16) \text{ \AA}]$. Both uranium and copper centers are thus 3-fold nodes, and the ligand is a 6-fold one. Here also, a 2D assembly, parallel to $(1\ 0\ \bar{1})$, is formed, which has the point symbol $\{4^3\}_2\{4^6.6^8.3^3\}$ (symbols for both uranium and copper, and L^{4-}

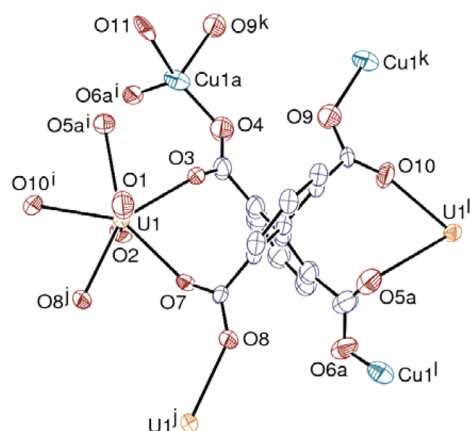


Figure 5. View of complex 4. Displacement ellipsoids are drawn at the 30% probability level. Only one position of the disordered atoms is represented. Solvent molecules and hydrogen atoms are omitted. Symmetry codes: $i = x, 3/2 - y, z - 1/2$; $j = 1 - x, 1 - y, 1 - z$; $k = 1 - x, 2 - y, 1 - z$; $l = x, 3/2 - y, z + 1/2$.

ligand, respectively), and is represented in nodal form in Figure 2. Doubly bridged uranyl dimers are present, each of which is bound to four L^{4-} ligands and is surrounded by four copper(II) cations. The two water ligands form hydrogen bonds with carboxylate acceptors in the same sheet and the lattice water molecule [O...O distances and O—H...O angles in the ranges 2.75(2)–3.04(2) Å and 118–169°, respectively]. As in complex 2, the ligand's main axis is perpendicular to the sheet plane.

Complex $[\text{UO}_2\text{Cu}(\text{L})(\text{H}_2\text{O})] \cdot \text{H}_2\text{O}$ (4) was obtained under conditions similar to those giving 3, but with acetonitrile being replaced by NMP as a cosolvent. The copper atom is disordered over two sites close to one another, as well as the carboxylate group bound to it (O5, O6) and the water ligands (see Supporting Information). The quite low resolution of the disordered parts results in uncertainties about the copper cation environment which, with only one water ligand, is close to distorted tetrahedral (Figure 5). Notwithstanding, and although these compounds crystallize in different space groups, the connectivity is identical to that in 3 and an analogous 2D network is formed.

In the additional presence of bipy, another heterometallic complex is obtained, $[(\text{UO}_2)_5\text{Cu}_4(\text{HL})_6(\text{bipy})_4] \cdot 2\text{H}_2\text{O}$ (5). It is notable that the synthesis of this complex is analogous to that of complex 1, with nickel(II) replaced by copper(II), but the 3d-block cation is not found as a separate counterion here. The asymmetric unit contains three uranyl ions, one of them (U3) with half-occupancy (see Supporting Information), two copper atoms and three HL^{3-} ligands (Figure 6). The three uranium atoms are in different environments: U1 is chelated in mode 2 by two ligands and bound to a fifth oxygen atom from a third ligand, U2 is chelated in mode 2 by one ligand only, chelated in mode 1 by another ligand, and bound to a fifth monodentate carboxylate donor, and U3 is chelated by two ligands in mode 1 and bound to a monodentate carboxylate. All three uranium atoms are in pentagonal bipyramidal environments, and they are all bound to three HL^{3-} ligands [U—O(carboxylate) bond lengths in the range 2.342(5)–2.577(15) Å; average 2.42(7) Å]. The copper atoms are in similar environments, being bound to three monodentate carboxylate oxygen atoms from three ligands and the chelating bipy molecule. In both cases, two oxygen atoms and the two nitrogen atoms are at distances of 1.954(5)–2.019(6) Å, while the other two oxygen atoms are at

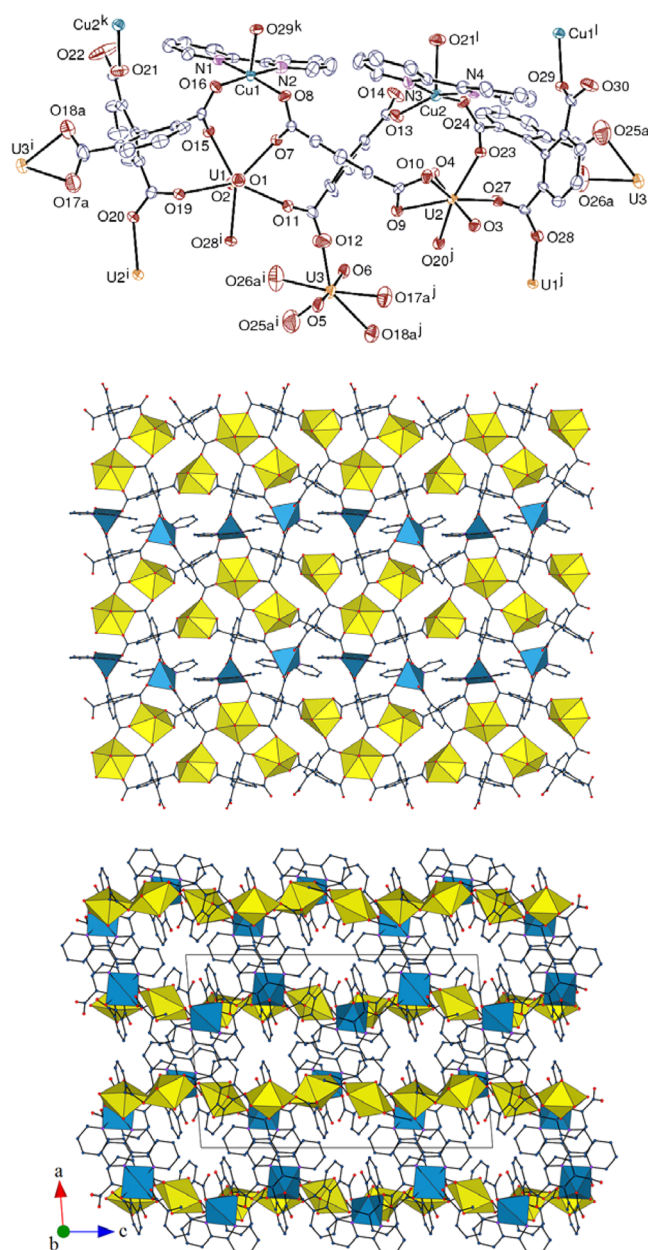


Figure 6. Top: View of complex 5. Displacement ellipsoids are drawn at the 50% probability level. Only one position of the disordered atoms is represented. Symmetry codes: $i = x, 1/2 - y, z - 1/2$; $j = x, 1/2 - y, z + 1/2$; $k = x, 3/2 - y, z - 1/2$; $l = x, 3/2 - y, z + 1/2$. Middle: View of the 2D assembly. Bottom: Packing with layers viewed edge-on. The uranium coordination polyhedra are yellow, and those of copper are blue. Solvent molecules and hydrogen atoms are omitted in all views.

greater distances of 2.254(5) and 2.355(6) Å, the environment being thus axially elongated square pyramidal. The three HL^{3-} ligands have the same coordination mode, chelating in both modes 1 and 2, and bound to three more metal cations in monodentate fashion, which makes them 5-fold nodes. The carboxylic protons have been found for two ligands only, and they are, as could be expected, on the single uncoordinated oxygen atom in each ligand. As in the previous complexes, a 2D assembly, parallel to (1 0 0), is formed. If the partial occupancy of atom U3 is disregarded (as it is in the nodal view in Figure 2 and the polyhedral representations in Figure 6), the network has the point symbol $\{4^2.6\}_3\{4^3\}_2\{4^4.6^4.8^2\}_3$ (successive

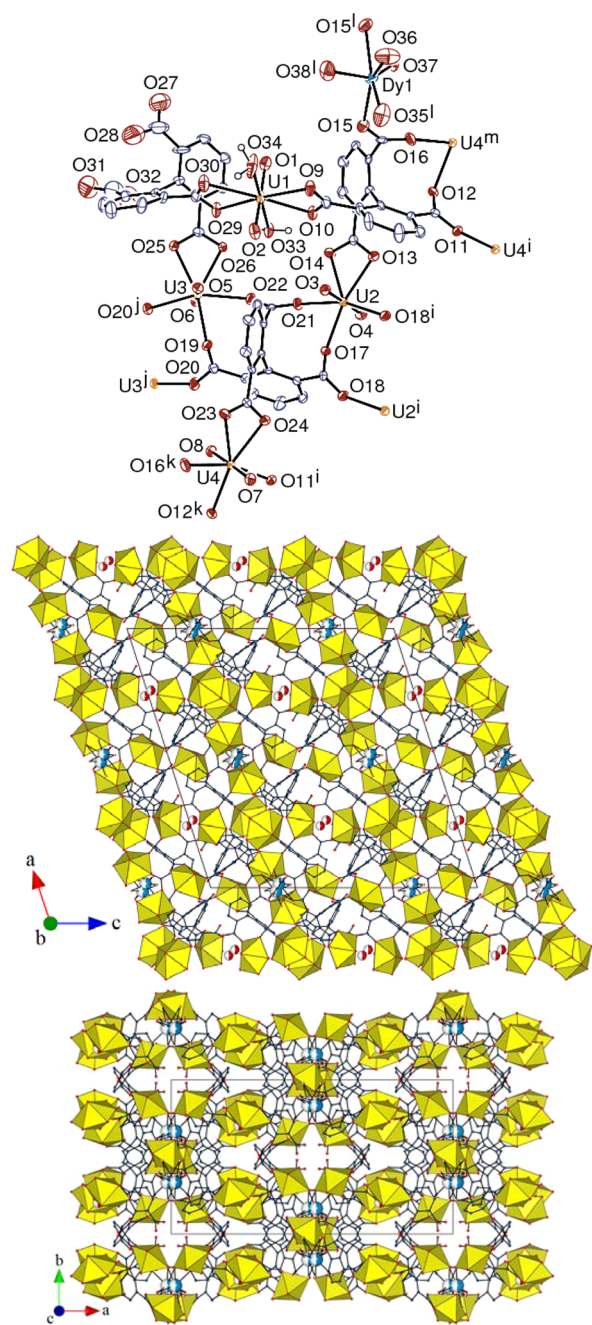


Figure 7. Top: View of complex **6**. Displacement ellipsoids are drawn at the 40% probability level. Only one position of the disordered atoms is represented. Counterions, solvent molecules and carbon-bound hydrogen atoms are omitted. Symmetry codes: $i = 1/2 - x, 3/2 - y, 1 - z$; $j = 1 - x, y, 3/2 - z$; $k = x + 1/2, y + 1/2, z$; $l = -x, y, 3/2 - z$; $m = x - 1/2, y - 1/2, z$. Middle and Bottom: Two views of the 3D framework. The uranium coordination polyhedra are yellow, and the disordered dysprosium and iodine atoms are shown as part-colored blue or red and white spheres, respectively. Solvent molecules and hydrogen atoms are omitted in the last two views.

symbols for U3/Cu1/Cu2, U1/U2 and the three HL³⁻ ligands). The layers display an alternation of rows of doubly bridged uranyl dimers with additional cations of the U3 family and rows of copper atoms. When viewed edge-on, these layers are not flat as those in the previous complexes **2–4** but gently undulating, with the bipy ligands directed outward on both sides. The HL³⁻ ligands are oriented nearly perpendicular to

the sheets, as in the previous cases. Aromatic stacking interactions, both inter- and intrasheet, may be present, with in each case one ring from HL³⁻ and one from bipy [centroid...centroid distances 4.003(5)–4.261(5) Å, dihedral angles 18.1(4)–26.1(4)°]. The carboxylic protons are hydrogen bonded to oxygen atoms from other ligands in the same sheet [O...O distances 2.481(9) and 2.666(8) Å, O–H...O angles 154 and 147°].

The last complex, [(UO₂)₈Dy(HL)₆(H₂O)₈](1)·8H₂O (**6**), pertains to the steadily growing family of heterometallic uranyl–lanthanide complexes.^{2f,h,21} Unobserved in the previous compounds in the present series, it includes iodide counterions present as an impurity resulting from the use of a very large excess of NaIO₄ during the synthesis of H₄L.⁸ The asymmetric unit contains four independent uranyl ions, a dysprosium(III) cation disordered over two positions close to one another (see Supporting Information), and three HL³⁻ ligands (the carboxylic protons were not found and HL³⁻ has to be considered as an average). Two different uranium environments are found: U1 is octa-coordinate with two chelating ligands in mode 1 and two water molecules in trans positions, while U2, U3, and U4 are chelated in modes 1 and 2 by two ligands and bound to a fifth carboxylic/ate oxygen atom from a third ligand, and they are thus seven-coordinate (Figure 7). The U–O(carboxylate) bond lengths are unexceptional [2.414(8)–2.559(8) Å, average 2.47(5) Å for mode 1 chelation, 2.319(8)–2.414(7) Å, average 2.35(3) Å for all other cases]. The disorder affecting the dysprosium atom and the water molecules bound to it prevent a description with precision of its coordination sphere, but it is sufficient for the present purposes to note that it is bound to two monodentate oxygen atoms (O15 and O15^l) from two ligands related to one another by a 2-fold rotation axis. From a topological point of view, U1 and Dy1 are thus 2-fold nodes, and U2, U3, and U4 are 3-fold nodes. The three HL³⁻ ligands display different coordination modes: one is twice chelating in mode 1 and once in mode 2, with two more monodentate coordinated oxygen atoms (5-fold node), another is twice chelated in mode 2 and once in mode 1, with two more monodentate coordinated oxygen atoms (5-fold node), and the last is chelated twice in mode 1, with one uncoordinated carboxylic/ate group on each ring (2-fold node). A 3D framework is formed, with the point symbol {4.6.8}–{4².6}–{4³.6².8³.10³.12².16²}–{4³.6².8⁴.10}–{4}–{6}–{6} (successive symbols for U3, U2/U4, two ligands, Dy1 and U1/last ligand, respectively), and it is shown in nodal form in Figure 2. As can be seen in Figure 7, no channel of significant size is formed, and the framework cannot be considered to display potential porosity.

Although the coordination mode of the present tetracarboxylic/ate ligand is quite variable (no particular mode is observed twice in the series, except in **3** and **4**, as shown in Scheme 2), it appears that mode 2 chelation associated with lateral bonding to two more cations is favored, being observed in all complexes (and also in several complexes with 3d-block transition metal cations^{11b,d,e,h,k}). The ligand displays this coordination mode twice in complexes **3** and **4** only, while it is associated with mode 1 chelation in **5** and **6**. In spite of possessing four divergent functional groups, a general tendency of this ligand is to form planar or quasi-planar architectures with uranyl ions and to adopt an orientation perpendicular to the sheets, which makes it a pseudoplanar ligand with the four coordinating groups at ~90° from one another. Only in the heterometallic complex **6** is this trend overcome and a 3D species obtained.

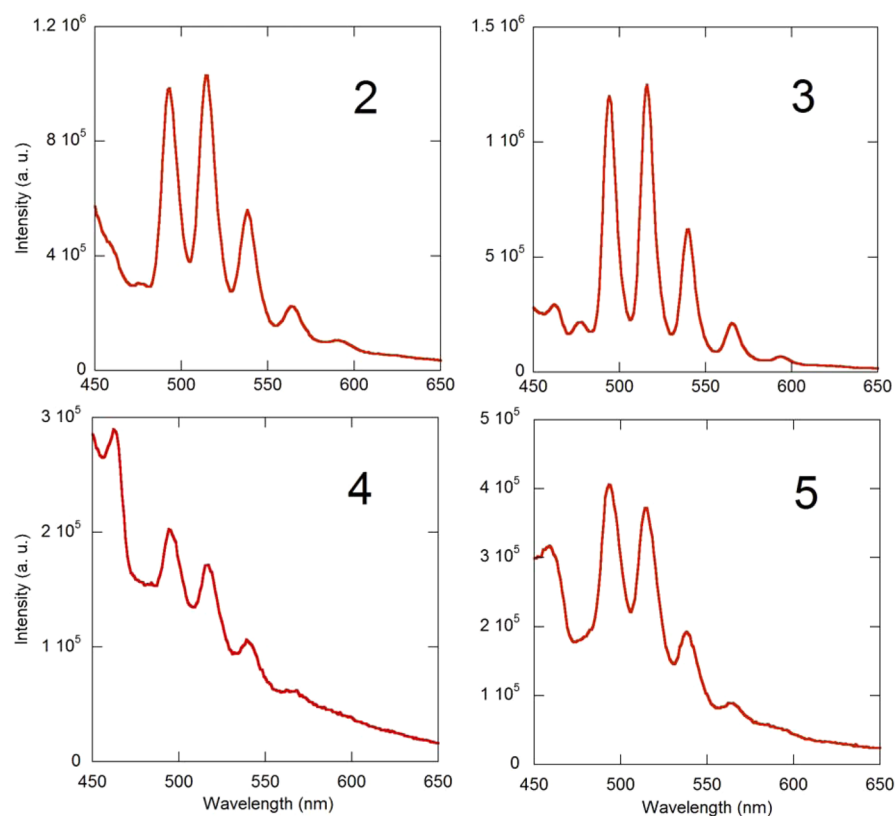


Figure 8. Solid state emission spectra of complexes 2–5. Excitation wavelength 420 nm.

From a purely topological viewpoint, the nodal representations given in Figure 2 point to an interesting similarity between some of these assemblies. The $\{4^2.6\}$ ribbon-like linear motif found in complex 1 also appears as a subunit in all complexes but for 3 and 4 (in which however similar subunits mixing uranium and copper centers can be found). These ribbons are connected to one another by $\text{UO}_2(\text{H}_2\text{O})_2^{2+}$ groups in complex 2, $\text{Cu}(\text{bipy})^{2+}$ groups in 5, and a more intricate, 3D bridging by both UO_2^{2+} and Dy^{3+} cations in 6. In this modest measure, it may be said that some predictability can be achieved with this ligand, although of course the finer details of structures involving a molecule with so many donor atoms defy prognostication.

Luminescence Properties. Emission spectra under excitation at a wavelength of 420 nm in the solid state were recorded for all compounds except 6, for which a sufficient quantity of crystals could not be isolated. The spectrum of complex 1 shows complete quenching of uranyl luminescence, which is indicative of energy transfer to the d–d excited state, followed by nonradiative decay, as observed in other cases;²² emission from $[\text{Ni}(\text{bipy})_3]^{2+}$ is not apparent in this case, in contrast to previous findings.^{22g} Complexes 2–5 display emission spectra, shown in Figure 8, with the typical vibronic progression corresponding to the $S_{11} \rightarrow S_{00}$ and $S_{10} \rightarrow S_{0\nu}$ ($\nu = 0–4$) electronic transitions.²³ While the spectra of the homometallic complex 2 and the $\text{UO}_2^{2+}/\text{Cu}^{2+}$ heterometallic complex 3 display intense and well resolved bands, those of the other $\text{UO}_2^{2+}/\text{Cu}^{2+}$ heterometallic complexes 4 and 5 are much less intense, probably due to partial quenching. The four main bands in all spectra are at 493–494, 514–516, 538–540, and 563–565 nm, which are values comparable to those found in other complexes with uranyl ions in an equatorial environment of five donor atoms.^{22c,e,g}

CONCLUSIONS

With its four divergent functional groups, the tetracarboxylic acid H_4L was initially considered a promising ligand for the formation of uranyl complexes having a 3D form. However, of the six complexes, either homo- or heterometallic, which have been obtained, five crystallize as quasi-planar 1D or 2D coordination polymers with the uranyl equatorial plane nearly parallel and the ligand main axis perpendicular to the assembly mean plane. This is not so surprising since the four carboxylic/ate groups are close to the plane bisecting the central bond of the ligand, which is nearly parallel to the assembly plane. In this respect and notwithstanding its very different shape, this ligand behaves in a similar way to flat polycarboxylates. It is interesting to note that 2D assemblies with ligands oriented in the same fashion as in complexes 1–5 have also been described with Mg^{2+} ,¹⁰ Co^{2+} ,^{11e} Ni^{2+} ,^{11a} Zn^{2+} ,^{11d,h,l} and In^{3+} .¹¹ⁱ The same tendency to form layers is also found in hydrogen bonded assemblies involving H_4L or its anions acting as square building blocks, some of them including also water molecules or ammonium cations.^{7b,9a,b,e} Only in the presence of Dy^{3+} cations was a 3D uranyl–organic framework obtained (complex 6), in which the three crystallographically independent carboxylic/ate ligands assume three different coordination modes. Although the latter are quite varied, with no two ligands adopting the same mode within the present series except in 3 and 4, chelation by two carboxylate groups, one from each aromatic ring, is a common feature. The chelated metal cation is located in the plane bisecting the central bond of the ligand, and this coordination mode is thus directly related to the formation of 2D networks. The emission spectra of complexes 1–5 in the solid state show either complete quenching due to the presence of a 3d-block metal cation, or emission bands of varying

intensity within the series, and with maxima positions similar to those of other uranyl ion complexes with five equatorial donors.

■ ASSOCIATED CONTENT

■ Supporting Information

Tables of crystal data, atomic positions, and displacement parameters, anisotropic displacement parameters, and bond lengths and bond angles in CIF format; crystal structure refinement details; infrared spectra; and excitation spectrum of 5. The Supporting Information is available free of charge on the ACS Publications website at DOI: 10.1021/acs.inorgchem.5b00596.

■ AUTHOR INFORMATION

Corresponding Authors

*(P.T.) E-mail: pierre.thuery@cea.fr.

*(J.H.) E-mail: harrowfield@unistra.fr.

Notes

The authors declare no competing financial interest.

■ REFERENCES

- (1) For an overview of uranyl–organic assemblies, see: (a) Cahill, C. L.; de Lill, D. T.; Frisch, M. *CrystEngComm* **2007**, *9*, 15–26. (b) Cahill, C. L.; Borkowski, L. A. In *Structural Chemistry of Inorganic Actinide Compounds*; Krivovichev, S. V., Burns, P. C., Tananaev, I. G., Eds.; Elsevier: Amsterdam, The Netherlands, 2007; Ch. 11. (c) Wang, K. X.; Chen, J. S. *Acc. Chem. Res.* **2011**, *44*, 531–540. (d) Andrews, M. B.; Cahill, C. L. *Chem. Rev.* **2013**, *113*, 1121–1136. (e) Loiseau, T.; Mihalcea, I.; Henry, N.; Volkringer, C. *Coord. Chem. Rev.* **2014**, *266*–*267*, 69–109. (f) Su, J.; Chen, J. S. *Struct. Bonding (Berlin)* **2015**, *163*, 265–296.
- (2) For some recent examples, see: (a) Liao, Z. L.; Li, G. D.; Wei, X.; Yu, Y.; Chen, J. S. *Eur. J. Inorg. Chem.* **2010**, 3780–3788. (b) Xia, Y.; Wang, K. X.; Chen, J. S. *Inorg. Chem. Commun.* **2010**, *13*, 1542–1547. (c) Mihalcea, I.; Henry, N.; Loiseau, T. *Cryst. Growth Des.* **2011**, *11*, 1940–1947. (d) Mihalcea, I.; Henry, N.; Clavier, N.; Dacheux, N.; Loiseau, T. *Inorg. Chem.* **2011**, *50*, 6243–6249. (e) Mihalcea, I.; Henry, N.; Volkringer, C.; Loiseau, T. *Cryst. Growth Des.* **2012**, *12*, 526–535. (f) Volkringer, C.; Henry, N.; Grandjean, S.; Loiseau, T. *J. Am. Chem. Soc.* **2012**, *134*, 1275–1283. (g) Mihalcea, I.; Henry, N.; Bousquet, T.; Volkringer, C.; Loiseau, T. *Cryst. Growth Des.* **2012**, *12*, 4641–4648. (h) Mihalcea, I.; Volkringer, C.; Henry, N.; Loiseau, T. *Inorg. Chem.* **2012**, *51*, 9610–9618. (i) Olchowka, J.; Falaise, C.; Volkringer, C.; Henry, N.; Loiseau, T. *Chem.–Eur. J.* **2013**, *19*, 2012–2022. (j) Olchowka, J.; Volkringer, C.; Henry, N.; Loiseau, T. *Eur. J. Inorg. Chem.* **2013**, 2109–2114. (k) Cantos, P. M.; Cahill, C. L. *Acta Crystallogr., Sect. E* **2014**, *70*, m142–m143. (l) Mihalcea, I.; Henry, N.; Loiseau, T. *Eur. J. Inorg. Chem.* **2014**, 1322–1332.
- (3) Cantos, P. M.; Jouffret, L. J.; Wilson, R. E.; Burns, P. C.; Cahill, C. L. *Inorg. Chem.* **2013**, *52*, 9487–9495.
- (4) Qu, Z. R. *Chin. J. Inorg. Chem.* **2007**, *23*, 1837–1839.
- (5) Thuéry, P.; Masci, B. *CrystEngComm* **2012**, *14*, 131–137.
- (6) Ji, C.; Li, J.; Li, Y.; Zheng, H. *Inorg. Chem. Commun.* **2010**, *13*, 1340–1342.
- (7) (a) Adams, R.; Yuan, H. C. *Chem. Rev.* **1933**, *12*, 261–338. (b) Holý, P.; Závada, J.; Císařová, I.; Podlaha, J. *Angew. Chem., Int. Ed.* **1999**, *38*, 381–383.
- (8) Pryor, K. E.; Shipps, G. W., Jr.; Skyler, D. A.; Rebek, J., Jr. *Tetrahedron* **1998**, *54*, 4107–4124.
- (9) See, for example: (a) Han, J.; Yau, C. W.; Lam, C. K.; Mak, T. C. W. *J. Am. Chem. Soc.* **2008**, *130*, 10315–10326. (b) Roy, S.; Mahata, G.; Biradha, K. *Cryst. Growth Des.* **2009**, *9*, 5006–5008. (c) Roy, S.; Biradha, K. *Cryst. Growth Des.* **2011**, *11*, 4120–4128. (d) Roy, S.; Mondal, S. P.; Ray, S. K.; Biradha, K. *Angew. Chem., Int. Ed.* **2012**, *51*, 12012–12015. (e) Roy, S.; Biradha, K. *Cryst. Growth Des.* **2013**, *13*, 3232–3241.
- (10) Dong, X. Y.; Hu, X. P.; Yao, H. C.; Zang, S. Q.; Hou, H. W.; Mak, T. C. W. *Inorg. Chem.* **2014**, *53*, 12050–12057.
- (11) See, for example: (a) Suh, M. P.; Moon, H. R.; Lee, E. Y.; Jang, S. Y. *J. Am. Chem. Soc.* **2006**, *128*, 4710–4718. (b) Huang, Y. G.; Gong, Y. Q.; Jiang, F. L.; Yuan, D. Q.; Wu, M. Y.; Gao, Q.; Wei, W.; Hong, M. C. *Cryst. Growth Des.* **2007**, *7*, 1385–1387. (c) Cheng, L.; Wang, J. Q.; Zhang, L. M. *Acta Crystallogr., Sect. E* **2010**, *66*, m1329. (d) Cheng, L.; Gou, S.; Zhang, L. *Solid State Sci.* **2010**, *12*, 2163–2169. (e) Cheng, L.; Wang, J. Q.; Gou, S. H. *Inorg. Chem. Commun.* **2011**, *14*, 261–264. (f) Chang, Z.; Zhang, D. S.; Hu, T. L.; Bu, X. H. *Inorg. Chem. Commun.* **2011**, *14*, 1082–1085. (g) Cheng, L.; Liu, F.; Gou, S. *Solid State Sci.* **2011**, *13*, 1542–1547. (h) Chang, Z.; Zhang, D. S.; Chen, Q.; Li, R. F.; Hu, T. L.; Bu, X. H. *Inorg. Chem.* **2011**, *50*, 7555–7562. (i) Xu, W. T.; Jiang, F. L.; Gao, Q.; Wu, M. Y.; Chen, L.; Hong, M. C. *Inorg. Chim. Acta* **2012**, *386*, 36–45. (j) Cheng, L.; Hu, H.; Zang, L.; Gou, S. *Inorg. Chem. Commun.* **2012**, *15*, 202–207. (k) Li, B.; Zang, S. Q.; Ji, C.; Hou, H. W.; Mak, T. C. W. *Cryst. Growth Des.* **2012**, *12*, 1443–1451. (l) Xuan, Z. H.; Zhang, D. S.; Chang, Z.; Hu, T. L.; Bu, X. H. *Inorg. Chem.* **2014**, *53*, 8985–8990.
- (12) Cheng, L.; Cao, Q.; Zhang, X.; Gou, S.; Fang, L. J. *Coord. Chem.* **2013**, *66*, 481–489.
- (13) Hooft, R. W. W. *COLLECT*; Nonius BV: Delft, The Netherlands, 1998.
- (14) Otwinowski, Z.; Minor, W. *Methods Enzymol.* **1997**, *276*, 307–326.
- (15) Sheldrick, G. M. *Acta Crystallogr., Sect. A* **2015**, *71*, 3–8.
- (16) (a) Sheldrick, G. M. *Acta Crystallogr., Sect. A* **2008**, *64*, 112–122. (b) Sheldrick, G. M. *Acta Crystallogr., Sect. C* **2015**, *71*, 3–8.
- (17) Farrugia, L. J. *J. Appl. Crystallogr.* **1997**, *30*, 565.
- (18) Momma, K.; Izumi, F. *J. Appl. Crystallogr.* **2008**, *41*, 653–658.
- (19) (a) Blatov, V. A.; Shevchenko, A. P.; Serezhkin, V. N. *J. Appl. Crystallogr.* **2000**, *33*, 1193. (b) Blatov, V. A.; O'Keefe, M.; Proserpio, D. M. *CrystEngComm* **2010**, *12*, 44–48.
- (20) (a) Allen, F. H. *Acta Crystallogr., Sect. B* **2002**, *58*, 380–388. (b) Bruno, I. J.; Cole, J. C.; Edgington, P. R.; Kessler, M.; Macrae, C. F.; McCabe, P.; Pearson, J.; Taylor, R. *Acta Crystallogr., Sect. B* **2002**, *58*, 389–397.
- (21) (a) Thuéry, P. *CrystEngComm* **2008**, *10*, 1126–1128. (b) Thuéry, P. *Inorg. Chem.* **2009**, *48*, 825–827. (c) Thuéry, P. *CrystEngComm* **2009**, *11*, 2319–2325. (d) Thuéry, P. *Cryst. Growth Des.* **2010**, *10*, 2061–2063. (e) Arnold, P. L.; Hollis, E.; White, F. J.; Magnani, N.; Caciuffo, R.; Love, J. B. *Angew. Chem., Int. Ed.* **2011**, *50*, 887–890. (f) Diwu, J.; Wang, S.; Good, J. J.; DiStefano, V. H.; Albrecht-Schmitt, T. E. *Inorg. Chem.* **2011**, *50*, 4842–4850. (g) Knope, K. E.; de Lill, D. T.; Rowland, C. E.; Cantos, P. M.; de Bettencourt-Dias, A.; Cahill, C. L. *Inorg. Chem.* **2012**, *51*, 201–206. (h) Thuéry, P. *CrystEngComm* **2012**, *14*, 3363–3366. (i) Thuéry, P. *CrystEngComm* **2012**, *14*, 6369–6373. (j) Hou, Y. N.; Xu, X. T.; Xing, N.; Bai, F. Y.; Duan, S. B.; Sun, Q.; Wei, S. Y.; Shi, Z.; Zhang, H. Z.; Xing, Y. H. *ChemPlusChem* **2014**, *79*, 1304–1315. (k) Thuéry, P. *Cryst. Growth Des.* **2014**, *14*, 2665–2676.
- (22) See, for example: (a) Alsobrook, A. N.; Zhan, W.; Albrecht-Schmitt, T. E. *Inorg. Chem.* **2008**, *47*, 5177–5183. (b) Heine, J.; Müller-Buschbaum, K. *Chem. Soc. Rev.* **2013**, *42*, 9232–9242. (c) Thuéry, P.; Harrowfield, J. *Cryst. Growth Des.* **2014**, *14*, 1314–1323. (d) Kerr, A. T.; Cahill, C. L. *Cryst. Growth Des.* **2014**, *14*, 1914–1921. (e) Thuéry, P.; Harrowfield, J. *CrystEngComm* **2014**, *16*, 2996–3004. (f) Thuéry, P.; Harrowfield, J. *Cryst. Growth Des.* **2014**, *14*, 4214–4225. (g) Thuéry, P.; Rivière, E.; Harrowfield, J. *Inorg. Chem.* **2015**, *54*, 2838–2850.
- (23) Brachmann, A.; Geipel, G.; Bernhard, G.; Nitsche, H. *Radiochim. Acta* **2002**, *90*, 147–153.